electrons) when uncoated preparations are examined. In addition the metallic marker permits good spatial resolution to be achieved in SEM[10].

Summary. A rapid method has been developed to visualize cell surface receptors in the SEM. Thus mannan at the surface of *Candida utilis* cells was localized by stabilized colloidal gold granules coated with either anti-mannan antibodies or Con A.

[10] Acknowledgment. We thank Mrs M. WEBER for the photographic work.

M. HORISBERGER, JAQUELINE ROSSET and H. BAUER

Research Department,
Nestlé Products Technical Assistance Co. Ltd.,
CH-1814 La Tour-de-Peilz (Switzerland),
16 June 1975.

Morphology of Colloidal Gold, Ferritin and Anti-Ferritin Antibody Complexes

Electron microscopical studies on the formation of ferritin – anti-ferritin complexes have been published previously[1–3]. Colloidal gold – ferritin mixtures have also been used to demonstrate membrane holes in osmotic and saponin hemolyses and membrane lesions in immune lysis[4, 5]. However, the structure of the complexes formed between colloidal gold particles, ferritin and anti-ferritin antibodies has not been studied in detail. It was therefore interesting to investigate the morphology of these complexes in order to evaluate their potential use as markers for transmission – and scanning-electron microscope cytochemical studies.

Experimental. The anti-ferritin antibodies were isolated by immunoadsorption from a colostral lactoserum of a cow immunized with horse spleen ferritin (cadmium free, 2× crystallized; Pentex Biochemicals). The presence of precipitating anti-ferritin antibodies was shown by a positive ring test[6] against a ferritin solution (1 mg/ml).

Ferritin and anti-ferritin antibodies were adsorbed onto colloidal gold according to the procedure of FAULK and TAYLOR[7], modified by GERBER et al.[8]. The colloids were suspended in phosphate-buffered saline, pH 7.2 to a final absorbance of 3.6 at 520 nm.

The different preparations were examined in a Philips EM 300 electron microscope after negative staining with 5% aqueous uranyl-acetate.

Results. In Figures 1–3 the individual materials used in our experiments are represented. The non-stabilized colloidal gold particles tend to aggregate (Figure 1). They have a polyhedrical form (inset) and are unstable under the electron beam. With progressive beam radiation, they become electron transparent (mass loss). The horse spleen ferritin (Figure 2) is quite homogeneous; however, some detached apoferritin (protein shell of the ferritin molecule) can be observed occasionally (arrow). The purified anti-ferritin antibodies (Figure 3) form small clusters of fairly constant diameter (30–40 nm). Aggregates of variable sizes of ferritin marked with colloidal gold granules (average diameter 5.2 nm) are visualized in Figure 4. Over 95% of the ferritin molecules are labelled with at least one gold particle. Adsorption of the gold colloid takes place onto the protein part of the ferritin molecules. Free apoferritin is therefore labelled as well. Figure 5 illustrates the purified anti-ferritin antibodies marked with colloidal gold. Most important is the observation that all colloid particles are covered by antibodies, i.e. after negative staining a clear, electron-transparent zone is visible around all colloidal gold granules. In favourable projections, the Y-shape of the anti-ferritin antibodies adsorbed onto the colloid particles can be revealed (Figure 5 simple arrow and inset). It is evident that this arrangement with the colloid granules in the center, surrounded by adsorbed immunprotein, is most favourable for immunocytochemical reactions. Small clusters of free antibodies (compare with Figure 3) are recognized occasionally (double arrows). Complexes between ferritin and colloidal gold, coated with anti-ferritin antibodies, are seen in Figure 6. They appear, due to the presence of antibodies, less densely packed than those formed by ferritin and uncoated colloidal gold. In this preparation, rather important fluctuations in the size of the colloid granules occurred. Finally, the rather heterogeneous complexes formed between ferritin marked with colloidal gold and colloidal gold covered with anti-ferritin antibodies are demonstrated in Figures 7 and 8. With adequate concentrations of ferritin and anti-ferritin antibodies, complexes of the type seen in Figure 7 are obtained. All ferritin molecules are surrounded by colloid particles, but it is impossible to distinguish between the gold granules directly adsorbed to the ferritin and those linked to the ferritin via the anti-ferritin antibodies. In Figure 7, the ferritin and anti-ferritin antibodies are not revealed because no negative staining was applied. Nevertheless, the ferritin nucleus (simple arrow) is easily distinguished from the gold particles (double arrow) by its considerably lower density. The same complexes after negative staining with uranyl acetate are shown in Figure 8. Again all the ferritin molecules are surrounded by colloid granules. The typical ferritin structure is masked (arrow) due to adsorption of antibodies. This is in agreement with observations on ferritin – anti-ferritin complexes[1].

Discussion. From the electron micrographs presented it is evident that mixed complexes are very heterogeneous in size and therefore not suitable as cytochemical markers. Two observations are, however, of importance. Firstly protein molecules are adsorbed around colloidal gold granules in a sterically favourable position necessary for cytochemical coupling or for the antibody-antigen reaction. This property has already been successfully exploited in labelling experiments in the transmission-[7–10] and

[1] A. FEINSTEIN and A. J. ROWE, Nature, Lond. *205*, 147 (1965).
[2] J. P. ROBINSON, J. molec. Biol. *17*, 456 (1966).
[3] J. P. ROBINSON and S. S. SCHUFFMAN, Immunology *20*, 883 (1971).
[4] P. SEEMAN, D. CHENG and G. H. ILES, J. Cell Biol. *56*, 519 (1973).
[5] G. H. ILES, P. SEEMAN, P. NAYLOR and B. CINADER, J. Cell Biol. *56*, 528 (1973).
[6] D. H. CAMPBELL, J. S. GARVEY, N. E. CREMER and D. H. SUSSDORF, in *Methods in Immunology* (W. A. Benjamin Inc., New York 1964), p. 131.
[7] W. P. FAULK and G. M. TAYLOR, Immunochemistry *8*, 1081 (1971).
[8] H. GERBER, M. HORISBERGER and H. BAUER, Infect. Immunity *7*, 487 (1973).
[9] H. BAUER, M. HORISBERGER, D. A. BUSH and E. SIGARLAKIE, Arch. Mikrobiol. *85*, 202 (1972).
[10] H. BAUER, D. R. FARR and M. HORISBERGER, Arch. Microbiol. *97*, 17 (1974).

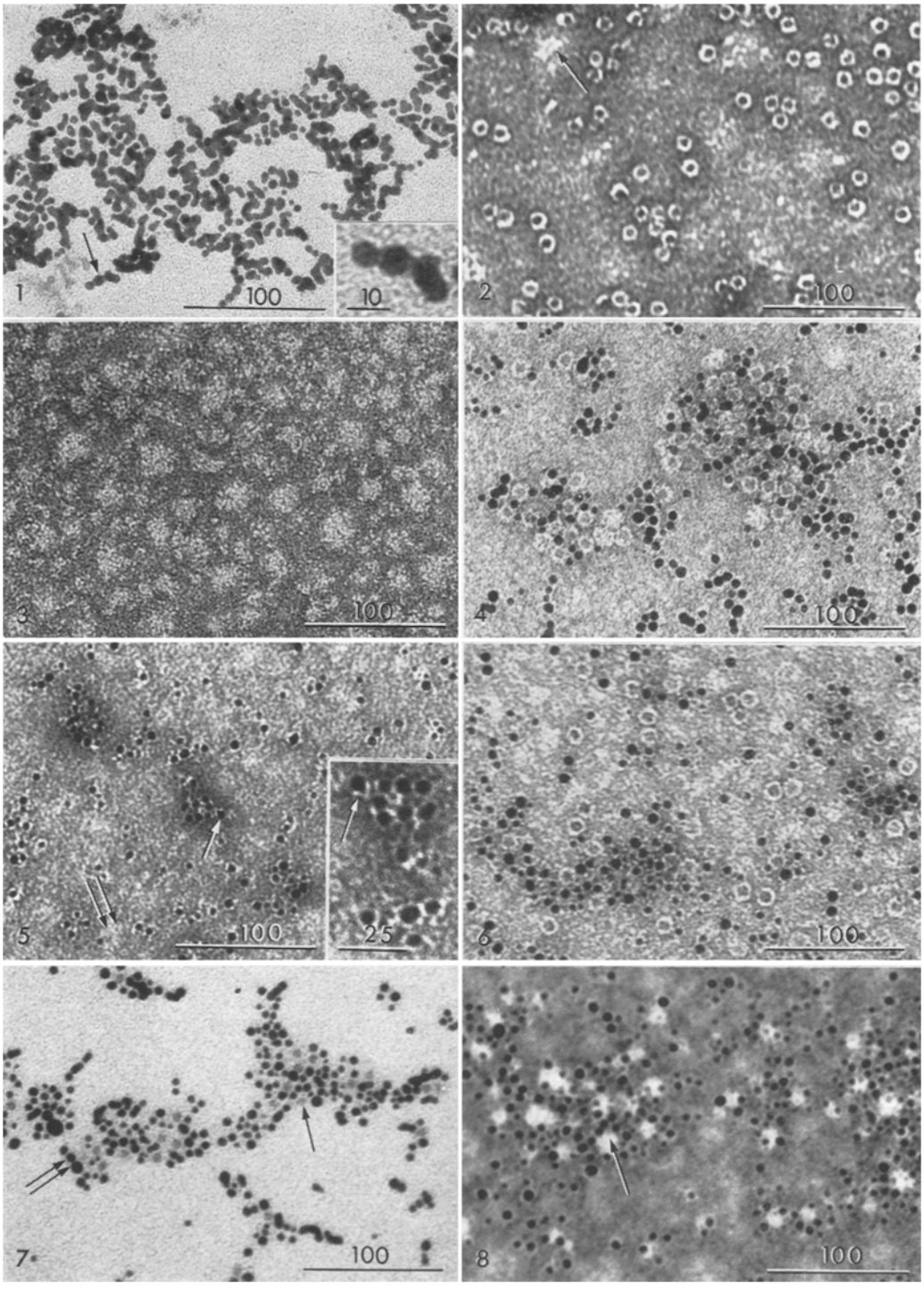

All electron micrographs, except Figure 7 (unstained), are from material negatively stained with 5% UO_2-acetate. The dimensions on the micrographs are given in nm.

Figs. 1–3. Individual materials used in our experiments. 1. Non-stabilized gold colloid particles showing instability under the electron beam. The polyhedrical form of the individual granules is well revealed (arrow, inset). ×250,000; inset ×500,000. 2. The horse spleen ferritin preparation is quite homogeneous. Some free apoferritin is indicated by an arrow. ×250,000. 3. The anti-ferritin antibodies tend to form small clusters of fairly constant diameter (30–40 nm). ×250,000.

Figs. 4 + 5. Direct marking of ferritin and anti-ferritin antibodies with colloidal gold. 4. The complexes formed between ferritin directly marked with colloidal gold are rather heterogeneous. Over 95% of the ferritin molecules are marked with at least one gold particle. ×250,000.

5. All colloid particles are coated with anti-ferritin antibodies. In favourable projections (arrow, inset), the Y-shape of the antibodies is revealed. The double arrow points to small cluster of free antibodies (comp. Figure 3). ×250,000; inset ×500,000.

Figs. 6–8. Marking of native and gold-labelled ferritin with anti-ferritin antibodies coated colloidal gold. 6. Complex formed between ferritin and colloidal gold coated with anti-ferritin antibodies. ×250,000. 7. Complexes formed between gold-labelled ferritin and colloidal gold coated with anti-ferritin antibodies. No negative staining was applied and therefore the protein part of the ferritin molecules and the anti-ferritin antibodies around the gold colloids is not revealed. Ferritin nucleus: ↓; gold particles: ↓↓. ×250,000. 8. Complexes formed between gold-labelled ferritin and colloidal gold coated with anti-ferritin antibodies. This preparation contains an excess of free antibodies, and it appears that free antibodies attach preferentially to the ferritin molecules (arrow). ×250,000.

recently in the scanning-[11] electron microscope. Secondly, even without negative staining, the gold colloid and the ferritin molecules (iron nucleus) can easily be detected and distinguished in the transmission electron microscope. Double labelling experiments, using colloidal gold particles coated with a protein (phytohemagglutinin, antibodies, etc.) and ferritin-protein conjugates can therefore be performed simultaneously.

Summary. The morphology of model complexes between colloidal gold, ferritin and anti-ferritin antibodies has been studied in order to evaluate the potential of colloidal gold as a cytochemical marker.

H. Bauer, H. Gerber[12] and M. Horisberger[13]

Research Department, Nestlé Products Technical Assistance Co. Ltd., CH-1814 La Tour-de-Peilz (Switzerland), and Pathology Institute, University of Berne, CH-3008 Berne (Switzerland), 16 June 1975.

[11] M. Horisberger, J. Rosset and H. Bauer, submitted for publication.

[12] Pathology Institute, University of Bern, CH-3008 Bern, Switzerland.

[13] Acknowledgment. We thank Prof. H. Isliker, Biochemistry Institute, University of Lausanne, for the bovine colostral antiserum against ferritin.

Hybridization of Mitochondrial and Cytoplasmic Ribosomal RNA with Mitochondrial and Nuclear DNA

The genetic origins of mitochondrial and cytoplasmic rRNAs from rat liver were investigated by RNA-DNA hybridization experiments. It was shown in earlier studies[1] that mitochondrial rRNAs from rat or mouse liver were different from their cytoplasmic counterparts in several of their physico-chemical properties. If in addition mitochondrial rRNAs hybridize specifically with mitochondrial DNA and not with nuclear DNA, this would be an indication of a different genetic origin from both types of rRNAs.

Material and methods. Mitochondria and RNA were prepared from adult rat liver as described in earlier studies[1]. During subcellular fractionation and RNA extraction, 2 ribonuclease inhibitors were used to avoid RNA degradation: a natural one prepared from rat liver the day before, and diethylpyrocarbonate. After ethanol precipitation, the RNAs were purified by 2 centrifugations through 5–20% sucrose gradients in order to completely eliminate tRNAs.

The cytoplasmic ribosomal RNAs were prepared according to Stevenin et al.[2], except that for the ribonuclease treatment, 0.05 µg ribonuclease per ml for 20 min at 0 °C was used to remove mRNA.

Mitochondrial DNA was prepared according to Ittel et al.[3] and the nuclear DNA according to Marmur[4], except that DNA was precipitated by cold ethanol and not by isopropanol. Both DNAs were fragmented by sonication as described by Mori et al.[5], in order to obtain fragments with a length of about 500 base pairs, which corresponds approximatively to a gene size[6,7]. The two species of DNAs were tritiated in vitro with sodium ^{3}H-borohydride as described by Lee and Gordon[8]. The specific activities of DNAs obtained varied from 5–1500 cpm/µg DNA.

The melting temperatures (Tms) of the DNA fragments and hybrids were determined by thermic elutions at increasing temperatures on hydroxyapatite columns. This method of temperature measurements[5] is very rapid and several determinations can be done simultaneously. Hydroxyapatite was prepared according to Tiselius[9] and modified by Levin[10]. The elution was performed with 0.12 *M* sodium phosphate buffer.

Nuclease S_1 was prepared according to Sutton[11] in our laboratory from takadiastase. Enzymatic activity was determined according to Sutton[11] except that the incubation was performed at 37 °C and not at 56 °C. This enzyme preferentially attacks single-stranded DNA.

Hybridization conditions were those of our laboratory. Tritiated DNA (12,000–15,000 cpm) was incubated with a large excess of RNA (100 to 600 times) in order to decrease strongly DNA-DNA reassociations, in 0.75 *M* sodium phosphate buffer for 48 h at 65 °C after heat denaturation. Hydroxyapatite (2 ml per column) was

Table I. Hybridization percentages of mitochondrial and cytoplasmic rRNAs with mitochondrial and nuclear DNA

	Mitochondrial DNA (% DNA hybridized)	Nuclear DNA (% DNA hybridized)
Mitochondrial rRNA	1.74 (10)	0.01 (3)
Cytoplasmic rRNA	0.02 (3)	0.42 (8)

The values in brackets are the number of determinations.

[1] A. Dierich, M. E. Ittel and M. Wintzerith, Life Sci. *13*, 553 (1973).

[2] J. Stevenin, J. Samec, M. Jacob and P. Mandel, J. molec. Biol. *33*, 777 (1968).

[3] M. E. Ittel, M. Wintzerith and P. Mandel, C. r. Acad. Sci., Paris, Série *D 274*, 3622 (1972).

[4] J. Marmur, J. molec. Biol. *3*, 208 (1961).

[5] K. Mori, M. Wintzerith and P. Mandel, Biochimie *54*, 1427 (1972).

[6] R. J. Britten and D. E. Kohne, Science *161*, 529 (1968).

[7] E. H. Davidson and B. R. Hough, Proc. natn. Acad. Sci., USA *63*, 342 (1969).

[8] V. F. Lee and M. P. Gordon, Biochim. biophys. Acta *238*, 174 (1971).

[9] A. Tiselius, S. Hjerten and O. Levin, Arch. Biochem. Biophys. *65*, 132 (1956).

[10] O. Levin, *Methods in Enzymology* (Eds. S. P. Colowick and N. O. Kaplan; Academic Press, New York 1962), vol. 5, p. 27.

[11] W. D. Sutton, Biochim. biophys. Acta *240*, 522 (1971).

Table II. Temperature values from nuclear and mitochondrial DNA, and RNA-DNA hybrids

	Temperature (°C)		Temperature (°C)
Mitochondrial DNA	82	Nuclear DNA	86
Mitochondrial DNA-mitochondrial rRNA hybrids	74.8	Nuclear DNA-cytoplasmic rRNA hybrids	78.5